Studies on Pathogenesis of Mitochondrial DNA with a Deletion in Mice

著者	堅田 俊
year	2014
その他のタイトル	マウス欠失突然変異型ミトコンドリアDNAの病原性発揮に関する基礎研究
学位授与大学	筑波大学 (University of Tsukuba)
学位授与年度	2013
報告番号	12102甲第6903号
URL	http://hdl.handle.net/2241/00123607

Studies on Pathogenesis of Mitochondrial DNA with a Deletion in Mice

January 2014

Shun KATADA

Studies on Pathogenesis of Mitochondrial DNA with a Deletion in Mice

A Dissertation Submitted to
the Graduate School of Life and Environmental Sciences,
the University of Tsukuba
in Partial Fulfillment of the Requirements
for the Degree of Doctor of Philosophy in Science
(Doctoral Program in Biological Sciences)

Shun KATADA

TABLE OF CONTENTS

ABSTRACT

Patient studies have suggested that the clinical phenotypes of some mitochondrial diseases might transit from one disease to another (e.g., Pearson syndrome [PS] to Kearns-Sayre syndrome [KSS]) in single individuals carrying mitochondrial (mt) DNA with a large-scale deletion (ΔmtDNA), but there is no direct experimental evidence for this. To determine if ΔmtDNA has the pathological potential to induce multiple mitochondrial disease phenotypes, I used *trans*-mitochondrial mice with a heteroplasmic state of wild-type mtDNA and ΔmtDNA (mito-miceΔ). Late-stage embryos carrying ≥50% ΔmtDNA showed abnormal hematopoiesis and iron metabolism in livers that were partly similar to PS (PS-like phenotypes), although they did not express sideroblastic anemia that is a typical symptom of PS. More than half of the neonates with PS-like phenotypes died by 1 month after birth, while the rest showed a decrease of ΔmtDNA load in the affected tissues, peripheral blood and liver, and they recovered from PS-like phenotypes. The proportion of ΔmtDNA in various tissues of the surviving mito-miceΔ increased with time, and KSS-like phenotypes were expressed when the proportion of ΔmtDNA in various tissues reached >70%-80%. My model mouse study clearly showed that a single ΔmtDNA was responsible for at least two distinct disease phenotypes at different ages and suggested that the level and dynamics of ΔmtDNA load in affected tissues would be important for the onset and transition of mitochondrial disease phenotypes in mice.

ABBREVIATIONS

B6	C57BL/6
COX	cytochrome *c* oxidase
ΔmtDNA	mitochondrial DNA with a large-scale deletion
E	embryonic day
KSS	Kearns–Sayre syndrome
mito-miceΔ	mice with ΔmtDNA
mtDNA	mitochondrial DNA
PEO	progressive external ophthalmoplegia
PS	Pearson syndrome

INTRODUCTION

Pathogenic mtDNAs having a large-scale deletion (ΔmtDNA) or a point mutation, induce defects of mitochondrial oxidative phosphorylation (mitochondrial respiration defects) and manifest a wide variety of mitochondrial diseases (Larsson and Clayton. 1995; Wallace. 1999). It has been well documented that ΔmtDNA is responsible for three clinical phenotypes of mitochondrial diseases: Kearns–Sayre syndrome (KSS), progressive external ophthalmoplegia (PEO), and Pearson syndrome (PS) (DiMauro and Garone. 2011). KSS is usually sporadic and is characterized by early onset (<20 years of age), lactic acidosis, chronic progressive external ophthalmoplegia, pigmentary retinopathy, heart block, diabetes, deafness, cerebellar abnormalities, and renal failure. PEO is mainly a skeletal muscle disorder and is characterized by late-onset progressive external ophthalmoplegia, lactic acidosis, myopathy, and exercise intolerance. PS is a rare disorder of early infancy that is characterized mainly by sideroblastic anemia. At present, the precise mechanism by which ΔmtDNA can cause different disease phenotypes is unclear, although it has been considered that different loads of ΔmtDNA in tissues are important to establish the multiple disease phenotypes.

Some patient studies have reported the possibility that infants with PS who survive into childhood develop the clinical features of KSS (Larsson *et al*. 1990; McShane *et al*. 1991; Rotig *et al*. 1995). Furthermore, Larsson and colleagues suggested that the transition of disease phenotypes is governed by the fractional concentration of ΔmtDNA in various tissues (Larsson *et al*. 1990); however, there is currently no experimental evidence for this. Since mitochondrial function is regulated both by nuclear DNA and mtDNA (Larsson and Clayton. 1995), it is possible that nuclear genomic background is involved in the pathogenesis of different disease phenotypes. Supporting evidence of this is the finding that the homoplasmic state of a pathogenic mutant mtDNA does not always induce serious clinical phenotypes in a mother and her children (McFarland *et al*. 2002).

Here, to experimentally resolve the question of whether mitochondrial disease phenotypes can change in single individuals due to the dynamics of the proportion of ΔmtDNA in various tissues, I have used a mouse model carrying pathogenic ΔmtDNA. Previously, my colleagues succeeded in generating a *trans*-mitochondrial mouse model (mito-miceΔ) with a heteroplasmic state for wild-type mtDNA and ΔmtDNA with a 4,696-bp deletion from nucleotide position 7,759 of the $tRNA^{Lys}$ gene to position 12,454 of the *ND5* gene (see Figure 1) (Inoue *et al*. 2000). The ΔmtDNA introduced in mito-miceΔ is similar to the pathogenic mutant mtDNA with the "common deletion" that is found in patients with KSS or PS (Holt *et al*. 1988; Larsson *et al*. 1990; McShane *et al*. 1991; Rotig *et al*. 1995). Since the mito-miceΔ all share the same nuclear genomic background (C57BL/6, also called B6), their genetic variation is restricted to the load of ΔmtDNA in various tissues. The mito-miceΔ, therefore, would provide the direct experimental evidence whether a single ΔmtDNA could cause the onset and transition of different mitochondrial disease phenotypes.

By using these mito-miceΔ, I investigated whether ΔmtDNA possesses a pathogenic potential for the onset of two distinct phenotypes of mitochondrial diseases, PS-like and KSS-like phenotypes, early in life (days 1−34 after birth) and in midlife (6 months of age), respectively. I also observed that the mice that escaped from the early death probably due to PS-like phenotypes developed KSS-like phenotypes in middle age, showing the transition of distinct mitochondrial disease phenotypes in single mito-miceΔ.

MATERIALS & METHODS

Mice

Thirty-three female mito-miceΔ carrying 1%–63% ΔmtDNA at 2–6 months of age were used as mothers. Embryos on E18.5 and progeny were used for the study. Age-matched wild-type B6 mice were used as normal controls. All animal experiments were performed in compliance with the institutional guidelines of the University of Tsukuba for the care and use of laboratory animals.

Estimation of ΔmtDNA proportion in tissues

Proportions of wild-type mtDNA and ΔmtDNA were determined by using real-time PCR, as described previously (Sato *et al*. 2005). Tail samples were used to deduce the ΔmtDNA load in mito-miceΔ. The proportion of ΔmtDNA was also examined in various tissue samples (peripheral blood, liver, kidney, and eye).

Cytological and histological analysis

Blood samples were smeared on glass slides, and inclusions in reticulocytes were visualized by staining with new methylene blue. Cells with granular network inclusions that are a typical structure of reticulocytes were counted (see open arrowheads in Figure 6A) and proportion of these reticulocytes to 1,000 red blood cells was estimated. The proportion of reticulocytes in blood samples of mito-miceΔ and age-matched controls was measured. To detect the accumulation of ferric iron, paraffin-embedded sections (5-μm thick) of liver samples were stained with Prussian blue and then Safranin O was used as a counter-staining. Eye samples were fixed in Bouin's solution, and paraffin-embedded sections (8-μm thick) of the samples were stained with hematoxylin and eosin.

Electron microscopic observation of COX activity

An electron microscopic analysis of COX activity was carried out as described previously (Nakada *et al*. 2001; Seligman *et al*. 1968) with slight modifications. Briefly, 25-μm cryosections of liver samples were fixed in 2% w/v glutaraldehyde in PBS for 5 min at 0°C. Ultrathin sections, which were not stained with uranyl acetate or lead nitrate solutions, were viewed directly on a transmission electron microscope (model H-7650, Hitachi High-Technologies Corporation, Tokyo, Japan). In this analysis, enzymatic activity of COX was visualized as a black color (high electron density).

Statistics

The Student's *t*-test was used to compare groups of data. All values are presented as means ± SD. The log-rank test was used to compare survival curves. *P* values less than 0.05 were considered to indicate statistical significance.

RESULTS

Frequency of early death in mito-miceΔ.

I first examined the early life spans (1–34 days after birth) of mito-miceΔ carrying 1%–70% ΔmtDNA in their tails (n = 126). The proportion of ΔmtDNA in individual mito-miceΔ was deduced from that in their tails just after birth (day 0). In this assay, I also used wild-type B6 mice as a normal control (n = 30). Approximately 20% of wild-type B6 neonates died on day 1 after birth (Figure 2A), but none died from days 2 to 34 (Figure 2B). The early life spans of mito-miceΔ carrying <50% ΔmtDNA in their tails were similar to those of wild-type B6 mice (Figure 2, B and C). In contrast, when the ΔmtDNA load in the neonates' tails was ≥50%, the frequency of death on day 1 after birth was definitely increased compared with that of wild-type B6 mice (Figure 2A). The mito-miceΔ carrying 50%–70% ΔmtDNA in their tails continued to die after day 1, and only 34% of these neonates survived until day 34 after birth (Figure 2D).

Although the above results indicated that most mito-miceΔ carrying ≥50% ΔmtDNA died early (≤34 days after birth), a substantial proportion of the progeny of mothers carrying >33% ΔmtDNA died very early (day 1 after birth) (Figure 3). Thus, it was unclear that early death was associated with the proportion of ΔmtDNA either in neonates or mothers. If the latter were the case, then the frequency of early death of pups would be expected to increase with the age of the mother, because ΔmtDNA accumulates in various somatic tissues but disappears in eggs with time (Sato *et al*. 2007). Therefore, I next examined the frequency of early death in the first and second litters of three female mito-miceΔ carrying 28% (Mouse 28), 52% (Mouse 52), and 61% (Mouse 61) ΔmtDNA, respectively, in their tails just after birth. As expected, the proportion of ΔmtDNA was much higher in the first litter than the second litter (Figure 4A). The rate of early death of pups was greatly and significantly higher in the first litter than in the second delivery (Figure 4, A and B, $P < 0.05$). The proportion of

surviving pups from the second litter (Figure 4B) was comparable to that of pups with wild-type B6 mothers (Figure 2A), despite the ΔmtDNA load of the mothers' tails increasing with time. Average loads of ΔmtDNA in tail samples were 32.4 ± 21.9% (mean ± SD) and 57.4 ± 16.8% in live and dead mito-miceΔ pups, respectively. Based on these results, I concluded that early death of mito-miceΔ was caused by ΔmtDNA load in neonates but not in mothers.

Phenotypic observations of late stage embryos of mito-miceΔ.

To clarify the reason for the frequent early death in progeny carrying ≥50% ΔmtDNA in their tails, I examined clinical phenotypes in embryos at embryonic day 18.5 (E18.5), which is just 1 day before birth. I obtained 55 E18.5 embryos carrying 35%–70% ΔmtDNA in their tails. I also examined 55 E18.5 embryos from wild-type B6 mice as a normal control. None of the E18.5 embryos of wild-type B6 mice showed lethal phenotypes. Among the E18.5 embryos from mito-miceΔ, three (5.5%) showed lethal phenotypes, and their tails carried 66%, 67%, and 70% ΔmtDNA, respectively, indicating that embryonic lethal phenotypes were restricted to embryos carrying a high load of ΔmtDNA. A typical example of an embryo with a lethal phenotype is shown in Figure 5A (right side): the embryo was atrophied and discolored when compared with littermate embryos carrying <66% ΔmtDNA in their tails. However, there was no significant difference in littermate number between normal mice and mito-miceΔ at E18.5 (Figure 5B). Thus, I concluded that the embryonic lethality was a rare event that was difficult to relate to the observation of frequent early death in mito-miceΔ.

I then examined the relationship between body weight and ΔmtDNA load in tails (Figure 5, A and C). The average body weight of wild-type E18.5 embryos was 1.19 ± 0.03 g

(n = 7), and that of E18.5 embryos carrying 34%–47% ΔmtDNA (1.20 ± 0.07 g, n = 8) was in the normal range. In contrast, a substantially lower body weight was seen in E18.5 embryos carrying 52%–66% ΔmtDNA (1.05 ± 0.13 g, n = 14, $P < 0.05$). Thus, growth retardation was induced preferentially in E18.5 embryos carrying ≥50% ΔmtDNA loads in tails, which was associated with frequent early death after birth. It is well known that ΔmtDNA is a genetic candidate for involvement in the pathogenesis of PS, which is a rapidly fatal disorder of infancy characterized mainly by sideroblastic anemia (DiMauro and Garone. 2011). My results suggested the possibility that neonates carrying ≥50% ΔmtDNA may show clinical phenotypes of PS. I therefore examined whether E18.5 embryos carrying ≥50% ΔmtDNA showed sideroblastic anemia. Typical sideroblasts were not observed in peripheral blood samples from E18.5 embryos carrying ≥50% ΔmtDNA. In contrast, compared with normal E18.5 embryos, the number of reticulocytes in peripheral blood samples from E18.5 embryos carrying ≥52% ΔmtDNA showed a statistically significant increase (Figure 6, A and B, $P < 0.05$), although the increase was slight. The proportion of reticulocytes in peripheral blood samples from E18.5 embryos carrying ≤42% ΔmtDNA was similar to that in samples from normal E18.5 embryos (Figure 6, A and B). These data suggested abnormalities of hematopoiesis and the resultant onset of mild anemia in E18.5 embryos carrying ≥50% ΔmtDNA. Because abnormal iron metabolism in liver is observed in cases of sideroblastic anemia and PS (Camaschella. 2008; Gurgey *et al*. 1996), I examined pathological changes in liver samples from E18.5 embryos carrying ΔmtDNA. Deposits of ferric iron indicating abnormal iron metabolism were preferentially observed in liver samples from E18.5 embryos carrying ≥50% ΔmtDNA (Figure 7). Based on these observations, I concluded that ≥50% ΔmtDNA loads could cause PS-like phenotypes in late-stage mouse embryos, although it was not a typical PS.

In previous studies of my colleagues using mito-miceΔ, accumulation of approximately 70%–80% ΔmtDNA loads in various tissues was necessary to induce mitochondrial respiration defects, such as deficiencies of complex IV (cytochrome *c* oxidase: COX) in mitochondrial respiratory chains, and the resultant onset of various clinical phenotypes. On the other hand, E18.5 embryos showed clinical phenotypes, even when they carried less than 70%–80% ΔmtDNA. These results suggest the possibility that threshold for tolerance to accumulation of ΔmtDNA in embryonic liver and blood cells would be lower than that in other tissues. Because electron microscopic observations of COX activity (COX-EM) can visualize COX activity in individual mitochondria of single cells (Nakada *et al*. 2001; Seligman *et al*. 1968), I next performed COX-EM with liver samples from E18.5 embryos carrying various loads of ΔmtDNA. In liver samples carrying ≥50% ΔmtDNA, I observed three types of mitochondria in a single cytoplasm of hepatocytes, mitochondrion that appeared normal in COX activity (arrows in Figure 8A), a swollen mitochondrion with COX activity (closed arrowhead in Figure 8A), and a COX-deficient swollen mitochondrion (open arrowhead in Figure 8A). In blood cells of liver samples carrying ≥50% ΔmtDNA, heterogeneity of COX activity within individual mitochondria was clearly visible (Figure 8B), although swollen mitochondria were not observed. These observations indicated that ≥50% ΔmtDNA loads could induce mitochondrial respiration defects in hepatocytes and blood cells of late-stage embryos. In addition, there were no autophagic double-membrane structures around abnormal mitochondria in hepatocytes or blood cells (Figure 8, A and B), indicating that that the COX-deficient mitochondria were not eliminated by the mitochondrial autophagy (mitophagy), even when a single cytoplasm contained mitochondria with different mitochondrial respiratory functions.

Changes of ΔmtDNA load and clinical phenotypes in mito-miceΔ during early life.

The results of the early life span described above (see Figure 2D) clearly showed that there were two populations of neonates carrying ≥50% ΔmtDNA in their tail; the first population showed death phenotypes in the first month after birth, probably due to PS-like phenotypes; and the second population were able to escape early death. In mito-miceΔ, genetic variation is restricted to the load of ΔmtDNA in various tissues, so that phenotypes are strictly induced by the load of ΔmtDNA in affected tissues. Considering this point, there was a possibility that the ΔmtDNA load decreased preferentially in the peripheral blood and liver of surviving neonates by around 1-month after birth. To test this possibility, I examined ΔmtDNA load in affected and non-affected tissues of surviving neonates at various time points up to and including day 34 after birth (Figure 9). In this assay, I could not trace the proportion of ΔmtDNA load in tissues from single neonates, because I had to sacrifice neonates to obtain tissue samples. Thus, I estimated the proportion of ΔmtDNA in each sample relative to that in the tail sample taken on day 0 after birth from the same subject. The animals were analyzed as two subgroups defined by the ΔmtDNA load in the tail (i.e,, <50% and ≥50% ΔmtDNA). In kidney samples as a non-affected tissue, the relative ratios increased with time in both subgroups, suggesting that the proportion of ΔmtDNA in the non-affected tissues increased independently of the ΔmtDNA load (Figure 9, $P < 0.05$). In peripheral blood, there were two distinct patterns dependent on ΔmtDNA load. In neonates carrying <50% ΔmtDNA in their tails at day 0, the relative ratios increased with time ($P < 0.05$) and the pattern was similar to that of kidney samples. In neonates carrying ≥50% ΔmtDNA in their tails at day 0, the relative ratios in peripheral blood samples did not increase with time. The relative ratios in liver samples from both subgroups did not increase with time. In the case of liver samples from E18.5 embryos carrying ≥50% ΔmtDNA, however, a significant decrease

of relative ratios was observed ($P < 0.05$).

To confirm changes in ΔmtDNA load in peripheral blood within same individuals, I collected peripheral blood samples from single neonates carrying 7%–64% ΔmtDNA, respectively, in their tails at day 0. I calculated the proportion of ΔmtDNA in peripheral blood on day 34 after birth relative to that on day 14 after birth (Figure 10). The relative ratios in surviving neonates carrying <50% ΔmtDNA in their tails were >1 and particularly high in neonates carrying <20% ΔmtDNA in their tails. In contrast, neonates carrying ≥50% ΔmtDNA in their tails showed relative ratios <1. There was a significant difference between neonates carrying <50% and ≥50% ΔmtDNA in their tails ($P < 0.05$). These data indicate that the proportion of ΔmtDNA in peripheral blood decreased at an early age (i.e., from days 14 to 34) when the proportion of ΔmtDNA in peripheral blood was ≥50%.

Consistent with these results, abnormalities observed in peripheral blood and liver samples of E18.5 embryos carrying ≥50% ΔmtDNA in their tails (Figure 6, 7 and 8A) were not detected on day 34 after birth (Figure 11–13). There was no significant difference in reticulocyte number between wild-type mice and mito-miceΔ (Figure 11, A and B). Iron deposits that were seen in livers from late stage embryos carrying ≥50% ΔmtDNA were not observed in the livers carrying 47% ΔmtDNA, which was the maximum proportion of ΔmtDNA observed on day 34 after birth (Figure 12) due to the decreased ΔmtDNA loads in liver. In COX-EM, abnormalities were not observed in liver samples (Figure 13). These findings indicate that the decrease of ΔmtDNA loading proportion in peripheral blood and liver of neonates carrying ≥50% ΔmtDNA in their tails would be one reason for recovering from PS-like phenotypes and for the resultant survival.

Disease phenotypes of surviving neonates when they reach middle life.

At 6 months of age or later, all the surviving mito-miceΔ showed lactic acidosis, heart block, renal failure, male infertility, deafness, and abnormalities in long-term memory as reported previously, when the proportion of ΔmtDNA in affected tissues reached approximately 70%-80% (Inoue *et al*. 2000; Nakada *et al*. 2001; Nakada *et al*. 2004; Nakada *et al*. 2006; Ogasawara *et al*. 2010; Tanaka *et al*. 2008). In some of surviving mito-miceΔ carrying >80% ΔmtDNA, retinal abnormalities were observed (Figure 14). These results indicated that neonates that remitted from PS-like phenotypes in early life expressed KSS-like phenotypes in their middle life.

DISCUSSION

Taking the current results together with previous studies of my colleagues, I summarized the development of mitochondrial diseases in mito-miceΔ (Figure 15). Based on the difference in ΔmtDNA loads and the resultant mitochondrial disease phenotypes, mito-miceΔ population is classified into four subgroups. The first subgroup is mito-miceΔ carrying ≤10% ΔmtDNA at the birth. They showed normal phenotypes, because ΔmtDNA loads did not reach >70%-80% in various tissues through the life (Normal subgroup in Figure 15). The second subgroup is mito-miceΔ carrying 11%–49% ΔmtDNA just after birth, and the mice appeared healthy until middle age (6 months) or later, but when the ΔmtDNA load reached >70%-80% in various tissues, they expressed KSS-like phenotypes (Late-onset subgroup in Figure 15). The main clinical features in this subgroup, such as low body weight, lactic acidosis, heart block, renal failure, deafness, male infertility, and abnormal long-term memory, has been reported previously (Inoue *et al*. 2000; Nakada *et al*. 2001; Nakada *et al*. 2004; Nakada *et al*. 2006; Ogasawara *et al*. 2010; Tanaka *et al*. 2008). The third and fourth subgroups are mito-miceΔ carrying ≥50% ΔmtDNA just after birth. When the ΔmtDNA load in late-stage embryos reached ≥50%, abnormalities of hematopoiesis and iron metabolisms in liver were induced, thus leading to PS-like phenotypes (i.e., abnormalities in hematopoiesis and iron metabolism; Figure 6 and 7), although >70%-80% ΔmtDNA loads were necessary for the onset of KSS-like phenotypes in adult mito-miceΔ. Half of those expressing PS-like phenotypes died in early life (≤34 days after birth). The third subgroup, therefore, was the case of onset of PS-like phenotypes and the resultant early death (Early-onset and death subgroup in Figure 15). The rest escaped from the early death, because PS-like phenotypes in them disappeared consistent with a decrease of ΔmtDNA load in affected tissues (see Figure 11 and 12 for the cases of peripheral blood and liver samples, respectively). However, they

expressed KSS-like phenotypes, when ΔmtDNA load reached >70%-80% in affected tissues (Figure 14). Thus, the fourth subgroup was the case of transient onsets of PS-like and KSS-like phenotypes in early and middle age, respectively, in a single mito-miceΔ (Early-and late-onsets subgroup in Figure 15).

Heterogeneous distribution of mitochondria with and without COX activity in single cells would be important for elucidating the reason why the pathogenic threshold load of ΔmtDNA in embryonic blood and liver was lower than that in other tissues. My colleagues have previously reported that a uniform distribution of mitochondria either with or without COX activity occurs in somatic cells of adult mito-miceΔ, irrespective of whether the tissues contain low or high loads of ΔmtDNA (Nakada *et al*. 2001). This indicates the occurrence of mitochondrial genetic complementation in which individual mitochondria exchange gene products derived from mtDNA through their fusion and fission. Because mitochondria carrying ΔmtDNA can be supplied by mitochondria carrying wild-type mDNA, tissues carrying ΔmtDNA did not show mitochondrial respiration defects until ΔmtDNA accumulated to a level of >70%-80%. In contrast, here I observed that blood cells and hepatocytes in late-stage embryos showing PS-like phenotypes contained mitochondria with heterogenous ultra-structures and COX activity levels (Figure 8, A and B). This finding suggested the existence of deficiencies of mitochondrial fusion or fission or both, and a lack of mitochondrial genetic complementation in these late-stage embryonic cells. Such deficiencies could be one reason that a load of ≥50% ΔmtDNA could cause pathogenicity in blood cells and hepatocytes of late-stage embryos, whereas a higher load is required in adult mice. Moreover, it has been reported that mitochondrial dynamics, a continuous mitochondrial fusion and fission, is necessary to maintain normal mitochondrial respiratory function in mammals (Chen *et al*. 2010; Ishihara *et al*. 2009). Therefore, it is possible that deficiencies of

mitochondrial dynamics and genetic complementation in embryonic blood cells and hepatocytes enhance the pathogenicity of ΔmtDNA in the case of a ≥50% ΔmtDNA load.

Interestingly, the significant increase in numbers of reticulocytes in peripheral blood samples from late-stage embryos with ≥50% ΔmtDNA, compared with those in normal controls, was not observed for 34-day-old mito-miceΔ with ≥50% ΔmtDNA (Fig. 11, A and B). Considering that mammalian hematopoiesis is classified into primitive and definitive forms, the latter of which is found in fetal liver and bone marrow after birth (Palis *et al*. 1998), my results suggested that hematopoietic cells locating in bone marrow showed a lower sensitivity to the accumulation of ΔmtDNA than those in embryonic liver. Thus, the change of hematopoietic organs from liver to bone marrow during early life could enable mito-miceΔ carrying ≥50% ΔmtDNA to escape death from PS-like phenotypes.

Because changes in the proportion of ΔmtDNA in affected tissues were highly associated with the development of different mitochondrial disease spectrums in mito-miceΔ, I propose that the dynamics of the ΔmtDNA load in affected tissues is one reason for the transition from PS-like to KSS-like phenotypes in single individuals. In this study, I observed two types of regulation in the dynamics of ΔmtDNA load (i.e., positive and negative). Accumulation of ΔmtDNA in various somatic cells (positive regulation), such as kidney, was considered responsible for the onset of KSS-like phenotypes in mito-miceΔ during middle life. Decreased ΔmtDNA load (negative regulation), was classified into two different modes of action. One was a ΔmtDNA load-dependent negative regulation that was seen in peripheral blood samples of mito-miceΔ in early life. With the recovery from PS-like phenotypes proceeded, there was a tendency that proportion of ΔmtDNA decreased in peripheral blood samples. Taking this finding together with the change of hematopoietic organs from liver to bone marrow during early life, the ΔmtDNA load-dependent negative regulation might be

necessary to remit from PS-like phenotypes. The other mode of action is the ΔmtDNA load-independent negative regulation that was seen in the liver of mito-miceΔ. In late-stage embryos and neonates of mito-miceΔ, the proportions of ΔmtDNA of liver were always lower than those in other embryonic tissues. The biological and clinical significance of this phenomenon remains to be answered.

Abnormal mitochondria are selectively degraded by autophagy, a process involved in protein and organelle turnover (Mizushima *et al*. 2008). Mitophagy is essential for biogenesis in yeast (Okamoto *et al*. 2009; Kanki *et al*. 2009), and experimental mitophagy in mammalian cultured cells is triggered by an acute disruption of the mitochondrial membrane potential (Narendra *et al*. 2008; Matsuda *et al*. 2010). The difference in individuality of each mitochondrion is considered to be a primary trigger for the occurrence of mitophagy in the vital state, so that it is possible that mitochondria with respiration defects are eliminated by mitophagy. Results of the COX-EM (Fig. 8, A and B), however, clearly showed that COX-positive and COX-negative mitochondria coexisted in single cytoplasms of blood cells and hepatocytes, and ultra-structural changes characteristic of mitophagy were not observed around COX-negative mitochondria. These findings suggested that the COX-negative mitochondria were not eliminated by the mitophagy, even when a single cytoplasm contained mitochondria with different mitochondrial respiratory functions. Consistent with this result, my colleagues previously observed a uniform distribution of COX-negative mitochondria without autophagic ultra-structures in cardiac muscle tissues and renal cells in the state of a high load of ΔmtDNA (Nakada *et al*. 2001). Therefore, chronic mitochondrial respiration defects induced by the accumulation of ΔmtDNA might be insufficient as a trigger for mitophagy, at least in the mammalian tissues examined here.

PS-like phenotypes induced by the abnormalities of hematopoiesis and iron

metabolisms in livers of late-stage embryos carrying ≥50% ΔmtDNA were the main clinical features, but it is unclear why a half of the neonates carrying ≥50% ΔmtDNA died early. There are several possible explanations for this phenomenon. The first is that the pups might have suffered acute oxidative stress, because newborns and infants are particularly prone to oxidative stress (Saugstad. 2005). Newborns and infants have reduced antioxidant defense mechanisms as well as high levels of free iron, which are required for the Fenton reaction (Saugstad. 2005); approximately 20% neonates died on day 1 after birth even in wild-type B6 mice (Figure 2, A and B). Since neonates carrying ≥50% ΔmtDNA in their tails possessed iron deposits in liver (Figure 7), the high level of iron could promote the Fenton reaction, resulting in additional oxidative stress when the neonates are exposed to a high oxygen concentration after delivery (Singer and Muhlfeld. 2007). Another possibility was that abnormalities in metabolic adaptation to the aerobic condition just after birth might cause frequent early death in mito-miceΔ. Anaerobic glycolysis is the major source of cellular ATP in fetal tissues. In cells with mitochondrial respiration defects due to pathogenic mutant mtDNAs, glycolysis is enhanced as a compensatory mechanism to maintain ATP levels. Therefore, ΔmtDNA might not demonstrate its pathogenicity in various cells during embryogenesis. Supporting this notion, I observed only rare incidents of embryonic lethality in mito-miceΔ. After birth, neonates carrying ΔmtDNA have to change from anaerobic to aerobic energy metabolism in various cells as soon as possible, but they would find this process difficult due to their systemic and chronic mitochondrial respiration defects.

In summary, my model mouse study showed that a single ΔmtDNA molecule has a pathogenic potential to cause PS-like and KSS-like phenotypes at early and middle life, respectively, and also suggested that difference in threshold for tolerance to accumulation of ΔmtDNA in affected tissues between young infants and adults is a possible reason for the

onset of disease phenotypes in mito-miceΔ. In addition, dynamics of ΔmtDNA load in affected tissues well correlated with the transition of disease phenotypes in mito-miceΔ. Considering that preferential accumulation of pathogenic mutant mtDNAs has been reported in some cases of cancer, diabetes, neurodegenerative diseases, and aging, the dynamics of pathogenic mtDNAs in affected tissues would cause a wide variety of mutant mtDNA-based disorders. Therefore, I believe that my findings will be of great interest in the field of genetics and medical sciences.

ACKNOWLEDGEMENTS

I thank Professor Kazuto Nakada and Professor Jun-Ichi Hayashi at the University of Tsukuba for their continuous guidance and valuable discussions through my doctoral program.

I would like to thank Professor Osamu Numata and Professor Tomoki Chiba at the University of Tsukuba for their review of my doctoral thesis.

Finally, I thank all of my colleagues at Professor Hayashi's laboratory for their support in this study and my family for their support of my life at the University of Tsukuba.

REFERENCES

Camaschella, C., 2008 Recent advances in the understanding of inherited sideroblastic anaemia. Br. J. Haematol. **143:** 27-38.

Chen, H., M. Vermulst, Y. E. Wang, A. Chomyn, T. A. Prolla *et al*, 2010 Mitochondrial fusion is required for mtDNA stability in skeletal muscle and tolerance of mtDNA mutations. Cell **141:** 280-289.

DiMauro, S., and C. Garone, 2011 Metabolic disorders of fetal life: Glycogenoses and mitochondrial defects of the mitochondrial respiratory chain. Semin. Fetal. Neonatal Med. **16:** 181-189.

Gurgey, A., I. Ozalp, A. Rotig, T. Coskun, G. Tekinalp *et al*, 1996 A case of pearson syndrome associated with multiple renal cysts. Pediatr. Nephrol. **10:** 637-638.

Holt, I. J., A. E. Harding and J. A. Morgan-Hughes, 1988 Deletions of muscle mitochondrial DNA in patients with mitochondrial myopathies. Nature **331:** 717-719.

Inoue, K., K. Nakada, A. Ogura, K. Isobe, Y. Goto *et al*, 2000 Generation of mice with mitochondrial dysfunction by introducing mouse mtDNA carrying a deletion into zygotes. Nat. Genet. **26:** 176-181.

Ishihara, N., M. Nomura, A. Jofuku, H. Kato, S. O. Suzuki *et al*, 2009 Mitochondrial fission factor Drp1 is essential for embryonic development and synapse formation in mice. Nat. Cell Biol. **11:** 958-966.

Kanki, T., K. Wang, Y. Cao, M. Baba, and D.J. Klionsky, 2009 Atg32 is a mitochondrial protein that confers selectivity during mitophagy. Dev. Cell **17:** 98-109.

Larsson, N. G., and D. A. Clayton, 1995 Molecular genetic aspects of human mitochondrial disorders. Annu. Rev. Genet. **29:** 151-178.

Larsson, N. G., E. Holme, B. Kristiansson, A. Oldfors and M. Tulinius, 1990 Progressive increase of the mutated mitochondrial DNA fraction in kearns-sayre syndrome. Pediatr. Res. **28:** 131-136.

Matsuda, N., S. Sato , K. Shiba, K. Okatsu, K. Saisho, *et al*, 2010 PINK1 stabilized by mitochondrial depolarization recruits parkin to damaged mitochondria and activates latent parkin for mitophagy. J. Cell Biol. **189:** 211-221.

McFarland, R., K. M. Clark, A. A. Morris, R. W. Taylor, S. Macphail *et al*, 2002 Multiple neonatal deaths due to a homoplasmic mitochondrial DNA mutation. Nat. Genet. **30:** 145-146.

McShane, M. A., S. R. Hammans, M. Sweeney, I. J. Holt, T. J. Beattie *et al*, 1991 Pearson syndrome and mitochondrial encephalomyopathy in a patient with a deletion of mtDNA. Am. J. Hum. Genet. **48:** 39-42.

Mizushima, N., B. Levine, A.M.Cuervo, and D.J. Klionsky, 2008 Autophagy fights disease

through cellular self-digestion. Nature **451:** 1069-1075.

Nakada, K., A. Sato, K. Yoshida, T. Morita, H. Tanaka *et al*, 2006 Mitochondria-related male infertility. Proc. Natl. Acad. Sci. U. S. A. **103:** 15148-15153.

Nakada, K., A. Sato, H. Sone, A. Kasahara, K. Ikeda *et al*, 2004 Accumulation of pathogenic DeltamtDNA induced deafness but not diabetic phenotypes in mito-mice. Biochem. Biophys. Res. Commun. **323:** 175-184.

Nakada, K., K. Inoue, T. Ono, K. Isobe, A. Ogura *et al*, 2001 Inter-mitochondrial complementation: Mitochondria-specific system preventing mice from expression of disease phenotypes by mutant mtDNA. Nat. Med. **7:** 934-940.

Narendra, D., A. Tanaka, D.F. Suen, and R.J. Youle, 2008 Parkin is recruited selectively to impaired mitochondria and promotes their autophagy. J. Cell Biol. **183:** 795-803.

Ogasawara, E., K. Nakada and J. Hayashi, 2010 Lactic acidemia in the pathogenesis of mice carrying mitochondrial DNA with a deletion. Hum. Mol. Genet. **19:** 3179-3189.

Okamoto, K., N. Kondo-Okamoto, and Y. Ohsumi, 2009 Mitochondria-anchored receptor Atg32 mediates degradation of mitochondria via selective autophagy. Dev. Cell **17:** 87-97.

Palis, J., and G.B. Segel, 1998 Developmental biology of erythropoiesis. Blood Rev., **12**, 106-114.

Rotig, A., T. Bourgeron, D. Chretien, P. Rustin and A. Munnich, 1995 Spectrum of mitochondrial DNA rearrangements in the pearson marrow-pancreas syndrome. Hum. Mol. Genet. **4:** 1327-1330.

Sato, A., K. Nakada, H. Shitara, A. Kasahara, H. Yonekawa *et al*, 2007 Deletion-mutant mtDNA increases in somatic tissues but decreases in female germ cells with age. Genetics **177:** 2031-2037.

Sato, A., T. Kono, K. Nakada, K. Ishikawa, S. Inoue *et al*, 2005 Gene therapy for progeny of mito-mice carrying pathogenic mtDNA by nuclear transplantation. Proc. Natl. Acad. Sci. U. S. A. **102:** 16765-16770.

Saugstad, O. D., 2005 Oxidative stress in the newborn--a 30-year perspective. Biol. Neonate **88:** 228-236.

Seligman, A. M., M. J. Karnovsky, H. L. Wasserkrug and J. S. Hanker, 1968 Nondroplet ultrastructural demonstration of cytochrome oxidase activity with a polymerizing osmiophilic reagent, diaminobenzidine (DAB). J. Cell Biol. **38:** 1-14.

Singer, D., and C. Muhlfeld, 2007 Perinatal adaptation in mammals: The impact of metabolic rate. Comp. Biochem. Physiol. A. Mol. Integr. Physiol. **148:** 780-784.

Tanaka, D., K. Nakada, K. Takao, E. Ogasawara, A. Kasahara *et al*, 2008 Normal

mitochondrial respiratory function is essential for spatial remote memory in mice. Mol. Brain **1:** 21.

Wallace, D. C., 1999 Mitochondrial diseases in man and mouse. Science **283:** 1482-1488.

FIGURES & FIGURE LEGENDS

Figure 1

Gene map of ΔmtDNA introduced in mito-miceΔ.

A wild-type mtDNA (left) is a circular DNA (16.3 kbp) and encodes 37 genes including 13 mRNAs, 22 tRNAs, and 2 rRNAs. A mtDNA with a large-scale deletion (ΔmtDNA; right) introduced in mito-miceΔ is 11.3 kbp in size, because 13 genes including 7 mRNAs and 6 tRNAs (arc) are lost by a deletion. Single capitals in maps indicate tRNA genes.

Figure 1

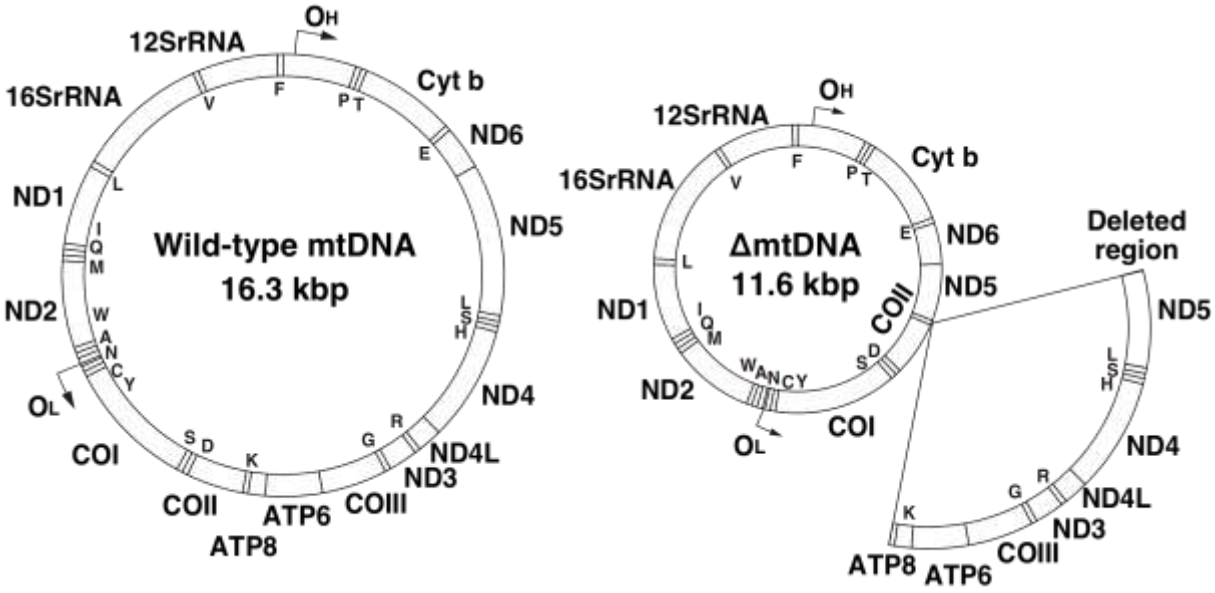
OH
12SrRNA
16SrRNA
Cyt b
ND6
ND1
ND5
Wild-type mtDNA
16.3 kbp
ND2
ND4
OL
COI
ND4L
ND3
COII
ATP6
COIII
ATP8
ΔmtDNA
11.6 kbp
Deleted
region

Figure 2

Observations of mito-miceΔ on the early life.

(**A**) Frequency of neonatal death in mito-miceΔ carrying 1%–70% ΔmtDNA in their tails. Neonates of mito-miceΔ were classified into four groups carrying 1%–34% (*n* = 23), 35%–49% (*n* = 30), 50%–59% (*n* = 42), and 60%–70% (*n* = 31) ΔmtDNA, respectively, in their tails. Neonates of wild-type B6 mice were used as normal controls (*n* = 30). (**B**)–(**D**) Life span of mito-miceΔ carrying 1%–70% ΔmtDNA in their tails was assessed for days 1 to 34. Based on the observed frequency of neonatal death in mito-miceΔ (see panel **A**), neonates of mito-miceΔ were classified into two groups carrying 1%–49% (*n* = 53) (**C**) and 50%–70% (*n* = 73) (**D**) ΔmtDNA in their tails, and the life span of each group was examined. The life span of wild-type B6 mice was also examined as a normal control (*n* = 30) (**B**). Survival curves were compared between mito-miceΔ carrying 1%–49% ΔmtDNA and wild-type B6 mice ($P = 0.3054$, log-rank test) and between mito-miceΔ carrying 50%–70% ΔmtDNA and wild-type B6 mice ($P < 0.0001$, log-rank test).

Figure 2

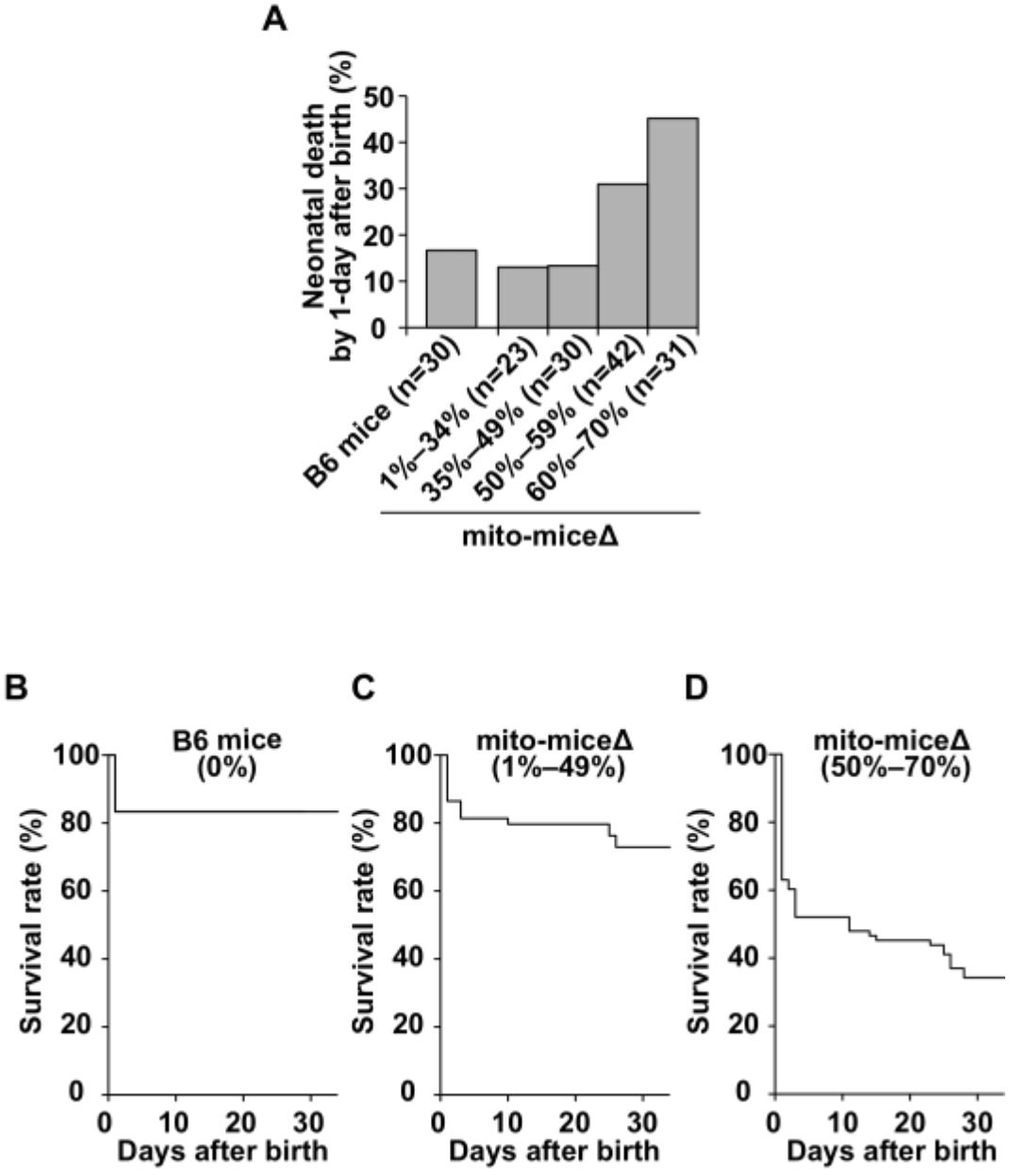
A
Neonatal death by 1-day after birth (%)
0
10
20
30
40
50
B6 mice (n=30)
1%–34% (n=23)
35%–49% (n=30)
50%–59% (n=42)
60%–70% (n=31)
mito-miceΔ
B
B6 mice (0%)
Survival rate (%)
Days after birth
C
mito-miceΔ (1%–49%)
Survival rate (%)
Days after birth
D
mito-miceΔ (50%–70%)
Survival rate (%)
Days after birth

Figure 3

Relationship between early death and ΔmtDNA load in mito-miceΔ.

Comparison of ΔmtDNA proportion in tail samples from pups and mothers. Open circles and red crosses indicate pups that were alive and dead, respectively, at 34 days after birth.

Figure 3

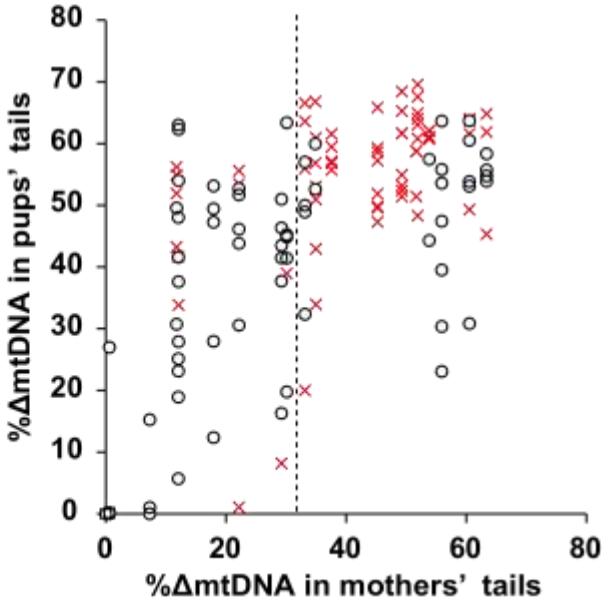
%ΔmtDNA in pups' tails
%ΔmtDNA in mothers' tails
0
10
20
30
40
50
60
70
80
0
20
40
60
80

Figure 4

The rate of early death in the first and second litters.

(**A**) Comparison between first and second litters in terms of pup survival and ΔmtDNA proportion in the tails of pups. Three female mito-miceΔ carrying 28% (Mouse 28), 52% (Mouse 52), and 61% (Mouse 61) ΔmtDNA in their tails just after birth (day 0) were used in this assay. Open circles and red crosses indicate the proportions of ΔmtDNA in the tails of pups that were alive and dead, respectively, at 34 days after birth. Blue symbols indicate the proportions of ΔmtDNA in mothers' tails. (**B**) Comparison between the first and second deliveries in terms of survival rates of pups from Mouse 28, Mouse 52, and Mouse 61 at day 34 after birth. Data are presented as mean ± SD. Asterisk indicates significant differences ($P < 0.05$).

Figure 4

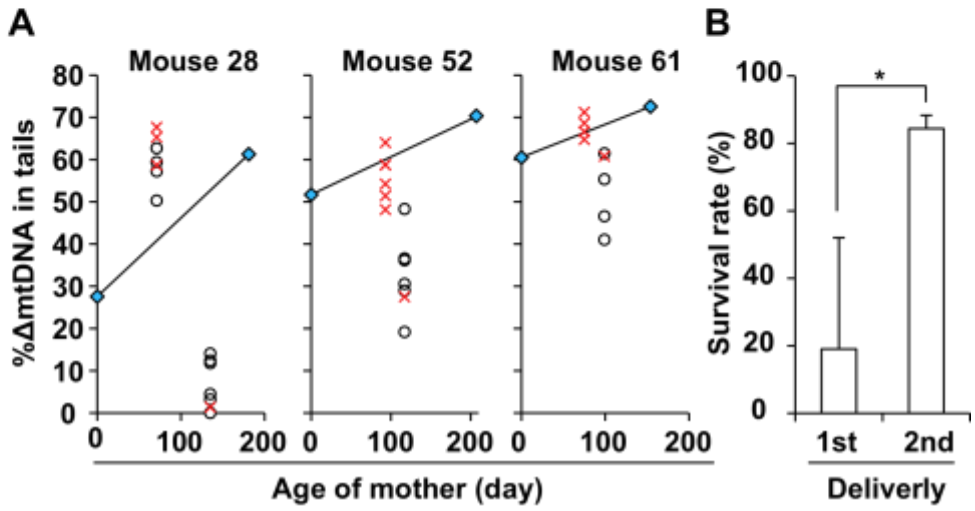
A
Mouse 28
Mouse 52
Mouse 61
%ΔmtDNA in tails
0
10
20
30
40
50
60
70
80
0
100
200
Age of mother (day)
B
Survival rate (%)
0
20
40
60
80
100
*
1st
2nd
Deliverly

Figure 5

Characteristics of late-stage embryos of mito-miceΔ.

All embryos were obtained at embryonic day 18.5. (**A**) Morphological observation of late stage embryos carrying 0%–66% ΔmtDNA in their tails, as indicated. The embryo carrying no ΔmtDNA (left side) was a wild-type B6 control. The six embryos carrying ΔmtDNA were obtained from a single mother. The weight of each embryo is shown below the panel. (**B**) Comparison of littermate number. Average numbers of littermates from 2-month-old female mito-miceΔ carrying 0% (white), 1%–32% (gray), or 33%–63% (black) ΔmtDNA. Data are presented as mean ± SD. NS, not significant. (**C**) Relationship between weight and ΔmtDNA load in late-stage embryos carrying 0% (white), 34%–47% (gray), or 52%–66% (black) ΔmtDNA. Data are presented as mean ± SD. Asterisks indicate significant differences ($P < 0.05$).

Figure 5

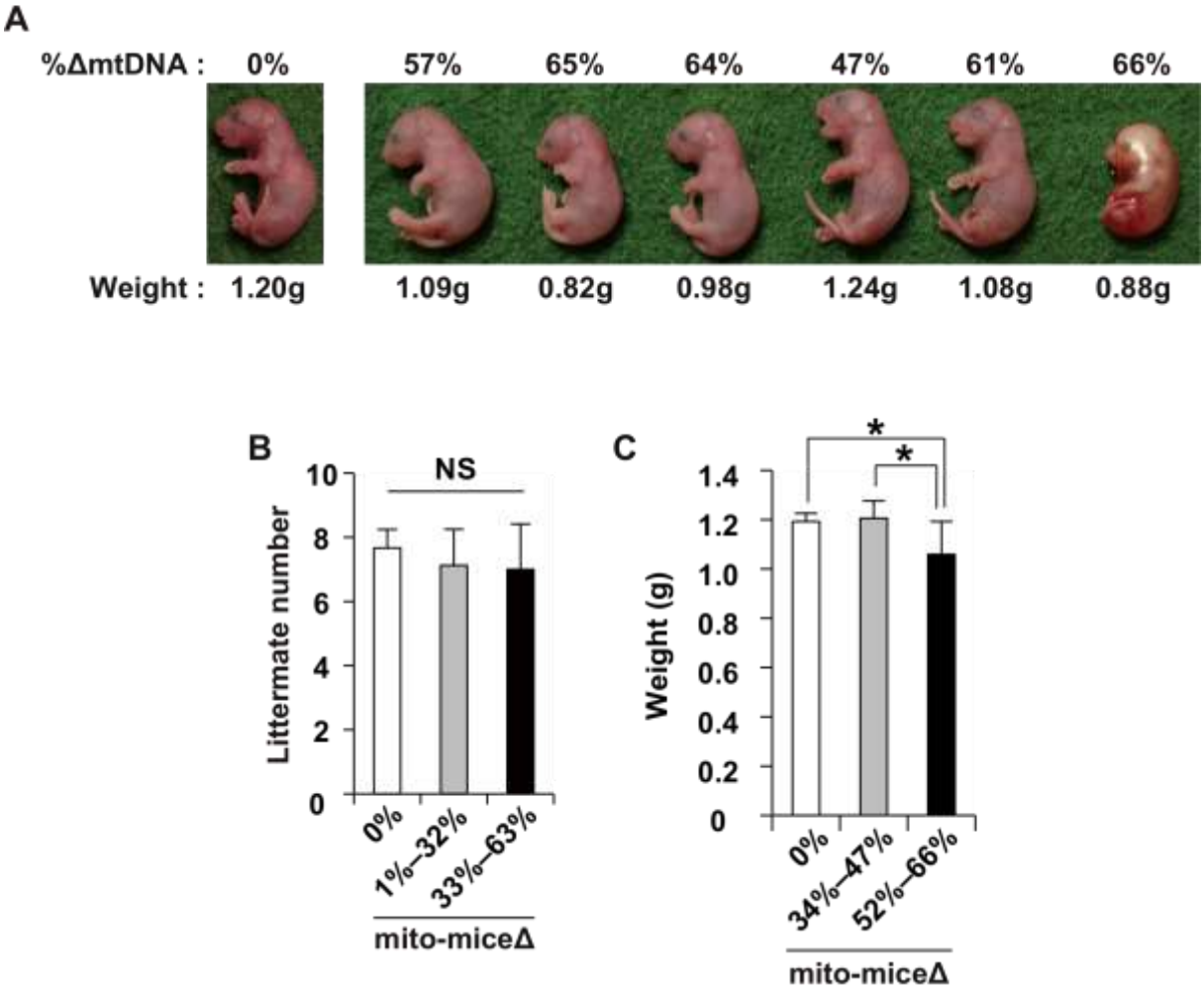
A
%ΔmtDNA :
0%
57%
65%
64%
47%
61%
66%
Weight :
1.20g
1.09g
0.82g
0.98g
1.24g
1.08g
0.88g
B
NS
Littermate number
10
8
6
4
2
0
0%
1%–32%
33%–63%
mito-miceΔ
C
*
*
Weight (g)
1.4
1.2
1.0
0.8
0.6
0.4
0.2
0
0%
34%–47%
52%–66%
mito-miceΔ

Figure 6

Hematological observations of late-stage embryos of mito-miceΔ.

(**A**) Hematological observation of peripheral blood samples from late-stage embryos. Peripheral blood samples carrying 0%, 36%, and 59% ΔmtDNA, respectively, were stained with new methylene blue. In this method, reticulocytes, a type of immature red blood cell (RBC), are visualized as cells with blue inclusions (open arrowheads). Scale bar, 10 μm. (**B**) Average proportion of reticulocytes in total RBCs in peripheral blood samples from late-stage embryos carrying 0% (white), 34%–42% (gray), or 52%–65% (black) ΔmtDNA. Data are presented as mean ± SD. Asterisks indicate significant differences ($P < 0.05$).

Figure 6

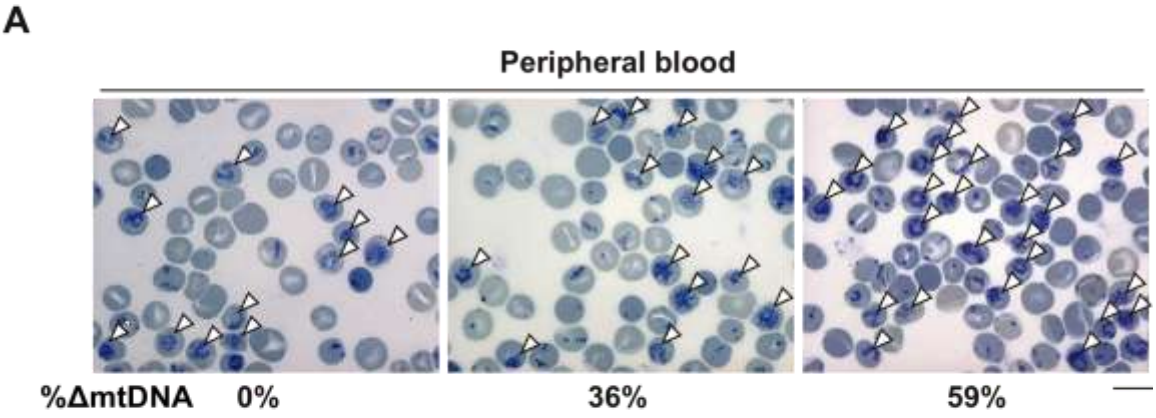
A
Peripheral blood
%ΔmtDNA 0%
36%
59%

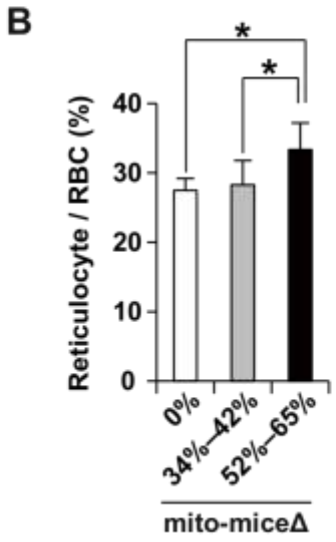
B
*
*
Reticulocyte / RBC (%)
40
30
20
10
0
0%
34%–42%
52%–65%
mito-miceΔ

Figure 7

Histological observations of late-stage embryos of mito-miceΔ.

Histological observations of iron metabolism in liver samples from late-stage embryos. Liver samples carrying 0%, 41%, and 55% ΔmtDNA, respectively, were stained with Prussian blue. In this method, abnormal iron metabolism is visualized as blue deposits. Scale bar, 10 μm.

Figure 7

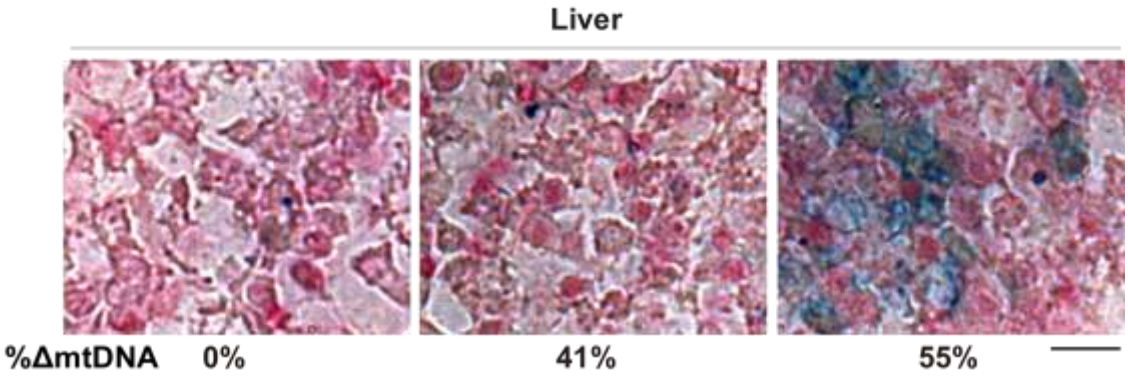

Figure 8

Electron microscopic observations of late-stage embryos of mito-miceΔ.

(**A**) and (**B**) Electron microscopic observations of COX activity in liver samples from late-stage embryos. Mitochondria in hepatocytes and blood cells are shown as (**A**) and (**B**), respectively. Arrows indicate mitochondria that appeared normal in shape and COX activity, open arrowheads indicate COX-deficient mitochondria, and the closed arrowheads indicate swollen mitochondria with COX activity. N, nucleus. Scale bar, 1 μm.

Figure 8

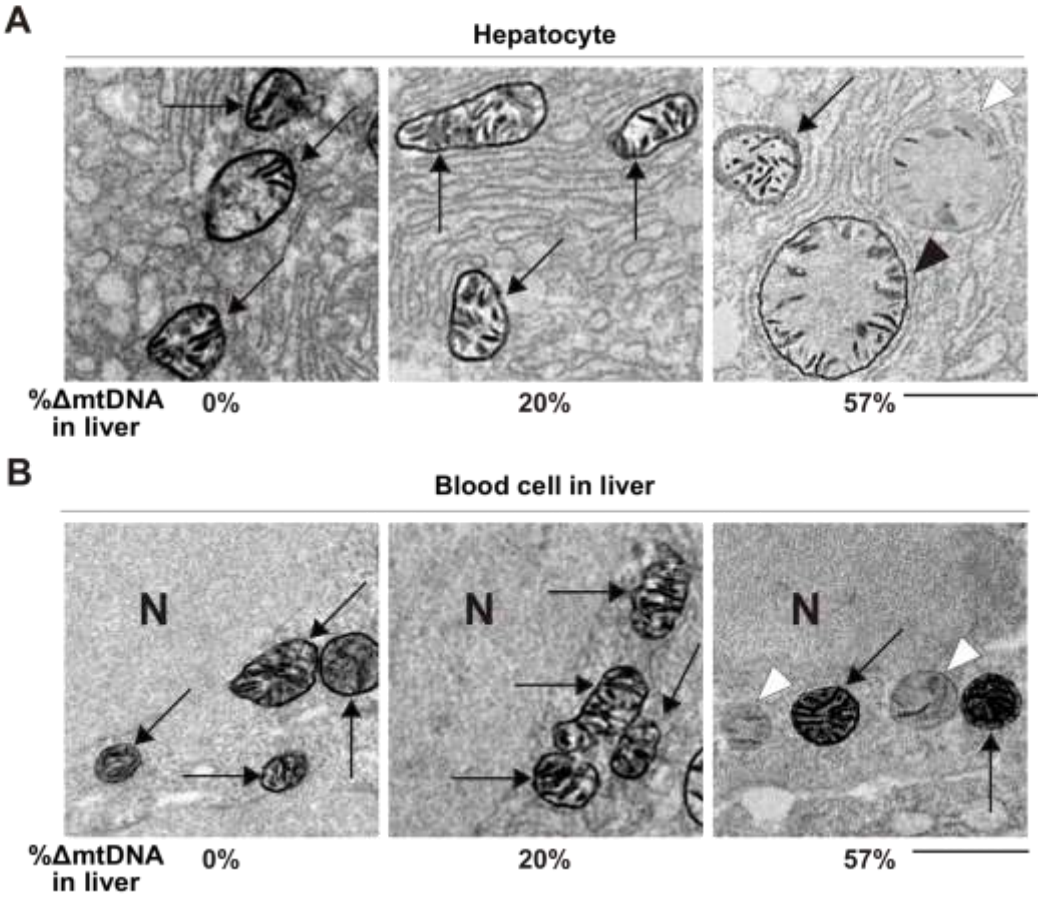
A
Hepatocyte
%ΔmtDNA in liver
0%
20%
57%
B
Blood cell in liver
N
N
N
%ΔmtDNA in liver
0%
20%
57%

Figure 9

Dynamics of the proportion of ΔmtDNA in early life of mito-miceΔ.

Dynamics of the proportion of ΔmtDNA in affected (peripheral blood and liver) and non-affected (kidney) tissues at various time points up to and including day 34 after birth. White and black bars indicate populations of mito-miceΔ carrying <50% and ≥50% ΔmtDNA in tail samples, respectively. The relative ratio is the proportion of ΔmtDNA in the tissue tested relative to that in the tail of the same individual at day 0 after birth. Data are presented as mean ± SD. Asterisks indicate significant differences ($P < 0.05$). NS, not significant.

Figure 9

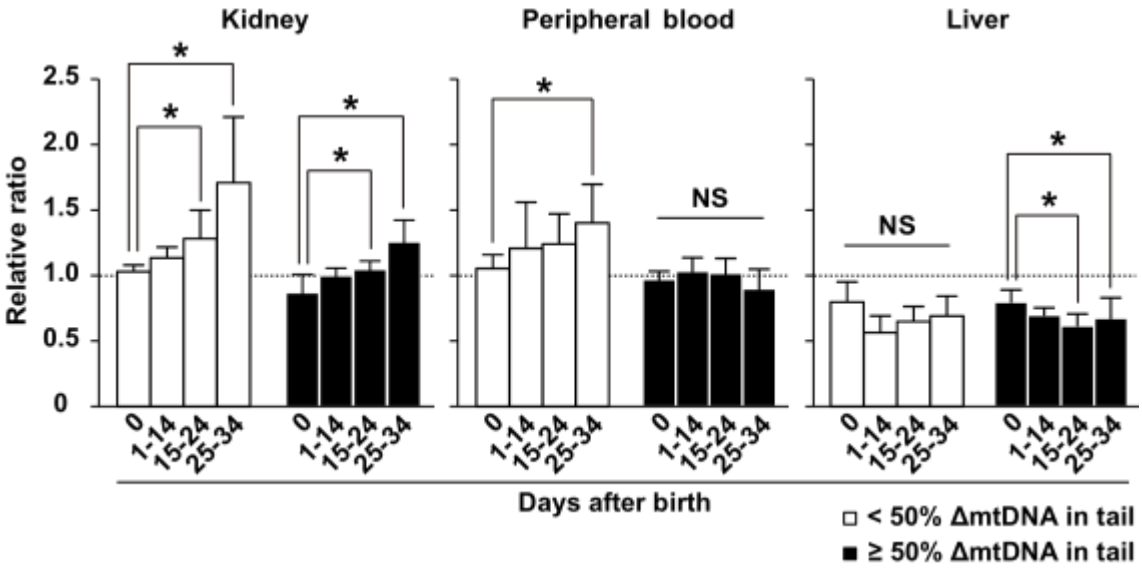
Kidney
Peripheral blood
Liver
Relative ratio
2.5
2.0
1.5
1.0
0.5
0
*
NS
0
1-14
15-24
25-34
Days after birth
□ < 50% ΔmtDNA in tail
■ ≥ 50% ΔmtDNA in tail

Figure 10

Dynamics of the proportion of ΔmtDNA in blood within the same individuals.

Dynamics of the proportion of ΔmtDNA in peripheral blood samples from single individuals during early life. Red and blue symbols indicate cases where the proportion of ΔmtDNA in peripheral blood samples increased and decreased, respectively, between days 14 and 34 after birth. Asterisk indicates significant differences ($P < 0.05$).

Figure 10

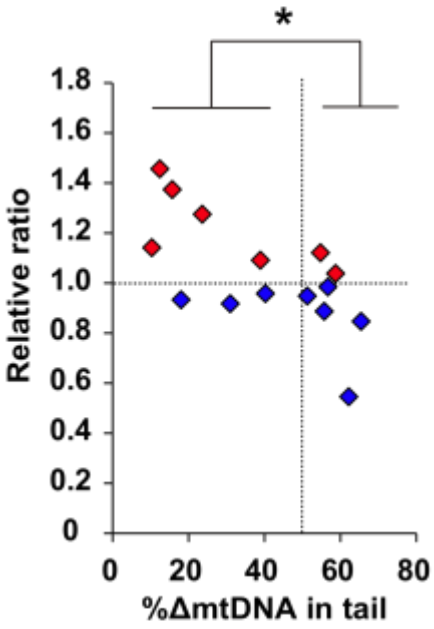
*
1.8
1.6
1.4
1.2
1.0
0.8
0.6
0.4
0.2
0
Relative ratio
0
20
40
60
80
%ΔmtDNA in tail

Figure 11

Hematological observations of mito-miceΔ at day 34 after birth.

(**A**) Hematological observations of peripheral blood samples obtained from mito-miceΔ at day 34 after birth. Peripheral blood samples carrying 0%, 38%, and 59% ΔmtDNA, respectively, were stained with new methylene blue and reticulocytes (open arrowheads) are visualized similar to Figure 6A. Scale bar, 10 μm. (**B**) Average proportions of reticulocytes in total RBC. Results for peripheral blood samples obtained from mito-miceΔ carrying 0%, 7%–38%, and 53%–64% ΔmtDNA are shown as white, gray, and black colors, respectively. Data are presented as mean ± SD. NS, not significant.

Figure 11

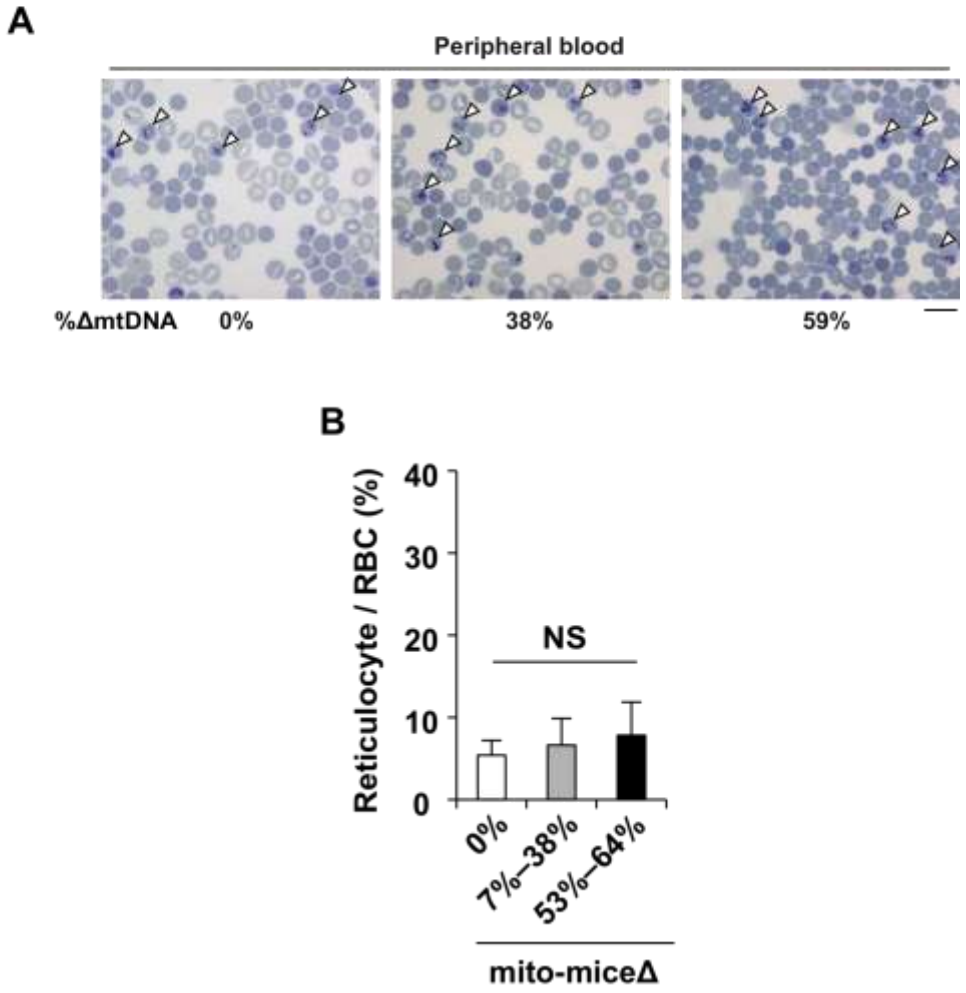
A
Peripheral blood
%ΔmtDNA
0%
38%
59%
B
Reticulocyte / RBC (%)
40
30
20
10
0
NS
0%
7%–38%
53%–64%
mito-miceΔ

Figure 12

Histological observations of mito-miceΔ at day 34 after birth.

Histological observations of iron metabolism in liver samples from mito-miceΔ at day 34 after birth. Liver samples carrying 0%, 38%, and 47% ΔmtDNA, respectively, were stained with Prussian blue. Scale bar, 10 μm.

Figure 12

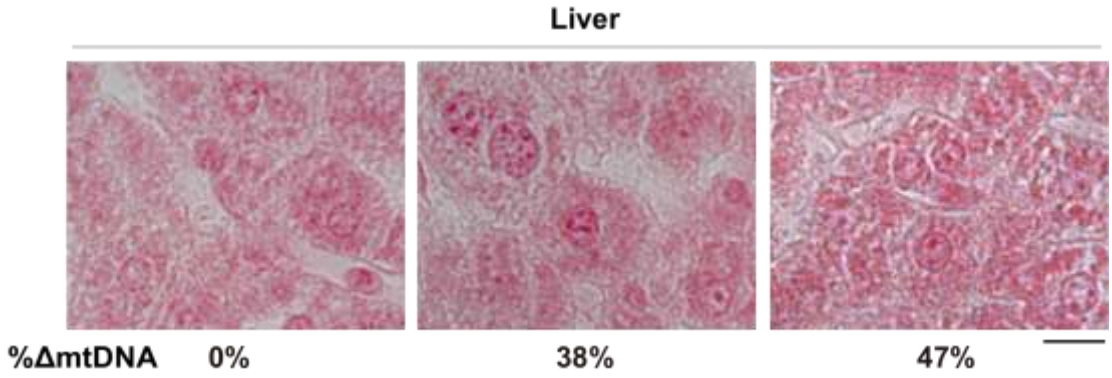

Figure 13

Electron microscopic observations of mito-miceΔ at day 34 after birth.

COX-EM of liver samples obtained from mito-miceΔ at day 34 after birth. The COX-EM of liver samples carrying 0%, 25%, and 47% ΔmtDNA, respectively, are shown. The loading of 47% ΔmtDNA was the maximum in the liver samples that I examined at day 34, because the proportion of ΔmtDNA in liver was lower than that in tissues during early life. N, nucleus. Bar, 2 μm.

Figure 13

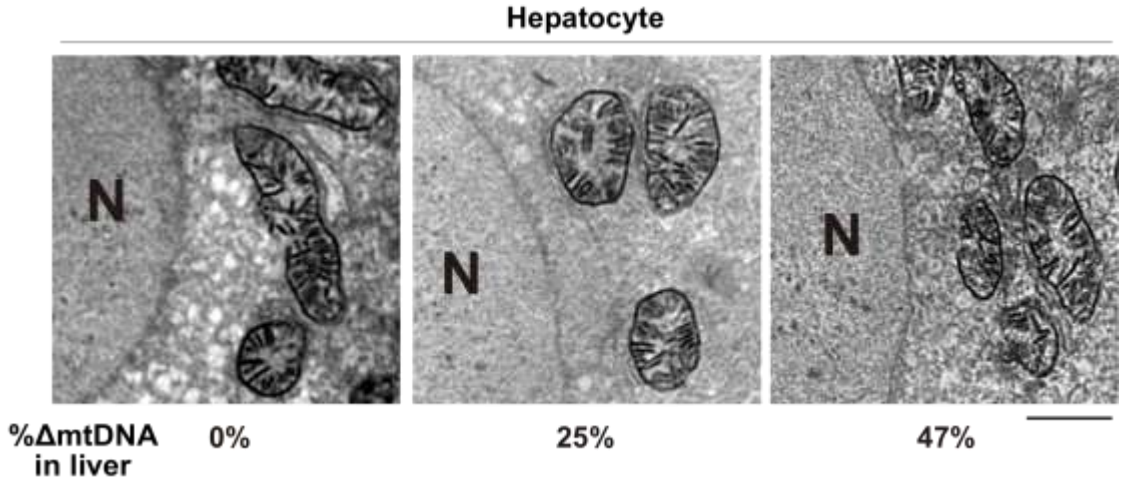

Figure 14

Phenotypic observations of middle-aged mito-mice∆.

Histological observations of retina from mito-mice∆ assayed at 6 months of age. Sections of eye samples were stained with hematoxylin and eosin. The proportion of ΔmtDNA in eye samples from the opposite side is indicated under the each picture. Scale bar, 50 μm.

Figure 14

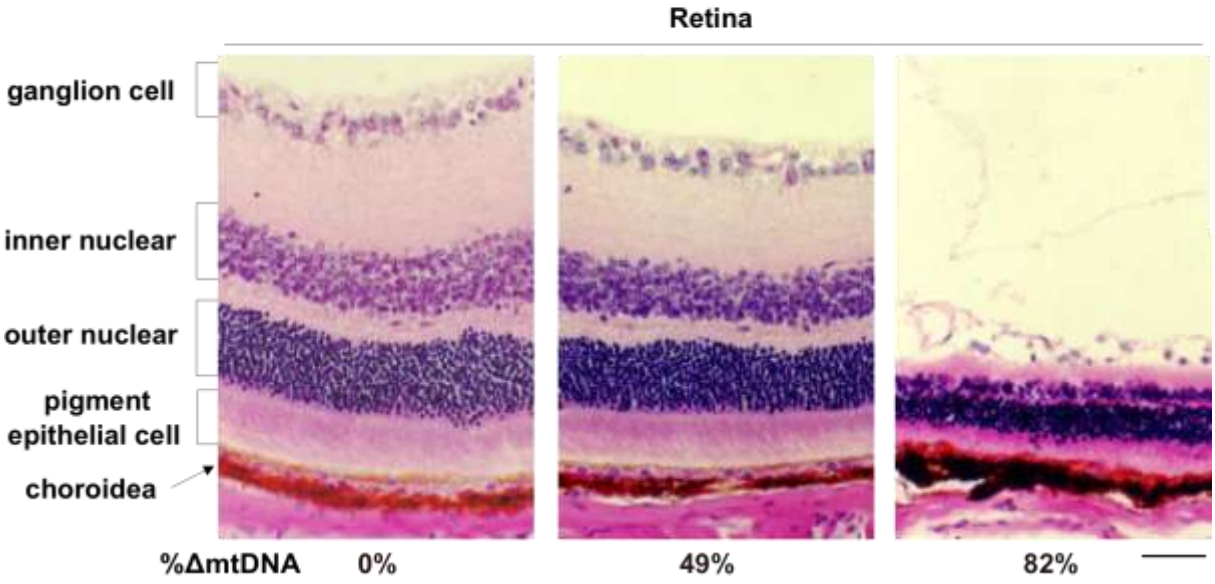
Retina
ganglion cell
inner nuclear
outer nuclear
pigment epithelial cell
choroidea
%ΔmtDNA
0%
49%
82%

Figure 15

Schematic representation of disease phenotypes in mito-miceΔ population.

"Normal" and "Late-onset" subgroups in mito-miceΔ populationn and their clinical features have already been reported as previous studies of my colleagues (Inoue *et al*. 2000; Nakada *et al*. 2001; Nakada *et al*. 2004; Nakada *et al*. 2006; Ogasawara *et al*. 2010; Tanaka *et al*. 2008). The novelty of this study was to found out two subgroups, "Early-onset and death" and "Early- and late-onsets" in addition of conventional two subgroups, "Normal" and "Late-onset" subgroups.

Figure 15

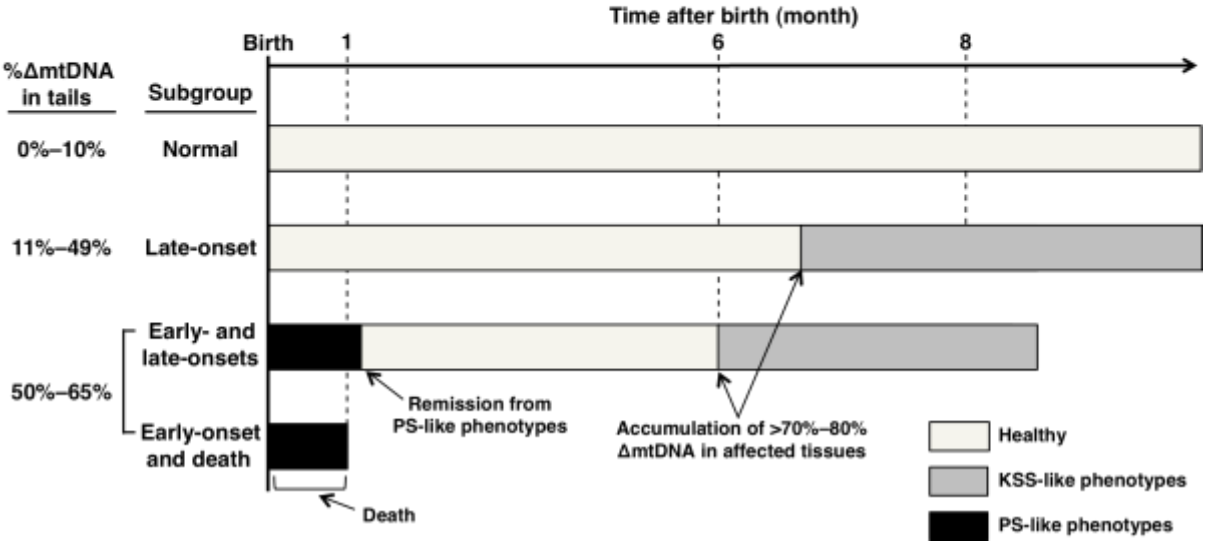
Time after birth (month)
Birth
1
6
8
%ΔmtDNA in tails
Subgroup
0%–10%
Normal
11%–49%
Late-onset
50%–65%
Early- and late-onsets
Early-onset and death
Remission from PS-like phenotypes
Accumulation of >70%–80% ΔmtDNA in affected tissues
Death
Healthy
KSS-like phenotypes
PS-like phenotypes